

Effect of the height of SCSW on the optimal position of the stiffening beam considering axial force effect

B. Farahmand Azar, A. Hadidi and H. Khosravi*

Faculty of Civil Engineering, University of Tabriz, Tabriz, Iran

(Received September 17, 2011, Revised December 19, 2011, Accepted January 3, 2012)

Abstract. Stiffened coupled shear walls (SCSW) are under axial load resulting from their weight and this axial load affects the behavior of walls because of their excessive height. In this paper, based on the continuum approach, the optimal position of the stiffening beam on the stiffened coupled shear walls is investigated considering the effect of uniformly distributed axial loads. Moreover, the effect of the height of stiffened coupled shear walls on the optimal position of the stiffening beam has been studied with and without considering the axial force effect. A computer program has been developed in MATLAB and numerical examples have been solved to demonstrate the reliability of this method. The effects of the various flexural rigidities of the stiffening beam on the internal forces and the lateral deflection of the structure considering axial force effect have also been investigated.

Keywords: stiffened coupled shear walls; continuous medium; optimal position; stiffening beam; axial force effect; closed-form solution

1. Introduction

Shear walls are commonly used in high rise buildings in order to increase the resistance of the structure against the lateral loads. They are formed as coupled shear walls because of the presence of openings constituted for the architectural aspects such as windows, doors etc. The behavior of coupled shear walls can be improved by incorporating stiffening beams at various levels. Continuous medium method has been extensively used for static and dynamic analysis of stiffened coupled shear walls. Using the continuous medium method, Coull (1974), Choo and Coull (1984) investigated the static behavior of coupled shear walls stiffened by a top and/or a bottom stiffening beam. The investigations showed that the presence of a stiffening beam could reduce the lateral deflection of the structure and relieve the bending stress in the walls. Adapting the same approach, Chan and Kuang (1989a, b) conducted studies on the effect of an intermediate stiffening beam at an arbitrary level along the height of the walls. Results of analysis indicate that the most favourable location for installing the stiffening beam is at the range of level from 0.2 to 0.5 of the structural height, depending on whether the achievement for the minimum value of the shear force in the lintel beams, or the bending moment in the walls at the base level, or the deflection at the top is to be made. Afterwards, Coull and Bensmail (1991) as well as Choo and Li (1997) extended Kuang

*Corresponding author, Ph.D. Student, E-mail: khosravi@tabrizu.ac.ir

and Chan's method for two and multi-stiffening beams. Their studies included both rigid and flexible foundations for the structure. Zeidabadi *et al.* (2004) indicated that the best location for the outrigger is usually somewhere between 0.4 to 0.6 of the height of the structure from the bottom. Hadidi *et al.* (2011) proposed a new method considering the effect of axial force for geometrically nonlinear analysis of the stiffened coupled shear walls.

For static analysis of stiffened coupled shear walls, the reader is referred for example to Arslan *et al.* (2001), Aksogan *et al.* (2003), Bikce *et al.* (2004), Bozdogan and Ozturk (2008), Emsen *et al.* (2009), among others. Kuang and Chau (1998), Arslan *et al.* (2004), Aksogan *et al.* (2007) have performed dynamic analyses on this type of shear walls.

In the research efforts expended so far on the effects of the various positions and rigidities of the stiffening beam on the results of static and dynamic analyses, the effect of axial force has not been considered. In a tall building, weight induced axial force can affect the behavior of the structure. In this paper, based on the continuum approach, the optimal position of the stiffening beam on the stiffened coupled shear walls is investigated considering the effect of uniformly distributed axial loads. Moreover, the effect of the height of stiffened coupled shear walls on the optimal position of the stiffening beam has been studied with and without considering the axial force effect. In the present research, it is assumed that the weight and axial force are uniformly distributed over the height of the wall. One of the main objectives of the present study is to determine that how much effect the axial force has on the realistic behavior of the stiffened coupled shear walls.

In this method, the discrete set of connecting beams has been initially replaced by a continuous medium and then the effects of the axial force on the lateral deformations have been taken into consideration. Afterwards, the equations of left and right axial forces in the walls, above and below the stiffening beam, have been derived. The governing differential equations for the deformation of stiffened coupled shear walls have been derived by setting up the equilibrium equations and the moment-curvature relationships for each wall with eliminating the laminar shear from the relationships. The closed-form solutions for these differential equations have been determined by applying the boundary conditions.

The main objective of the present research is to derive the differential equations governing the behavior of the stiffened coupled shear walls, considering the effect of the axial force. Furthermore, this method investigates the effects of different flexural rigidities of the stiffening beam to obtain the optimal position for the lateral deflection and base bending moment of the structure considering the axial force effect. The comparison of results has been carried out for the optimal position of the stiffening beam on the stiffened coupled shear walls with and without considering the axial force effect.

2. Method of analysis

Due to the high in-plane stiffness of the floors, it is assumed that connecting beams do not experience any axial deformations. Thus, both shear walls will have the same lateral displacements and the curvature throughout their height. A typical stiffened coupled shear walls is shown in Fig. 1. In this figure, the stiffening beam has been placed at the height of h_s and the other specifications and parameters of the wall have also been shown. Based on the continuum approach of analysis, the discrete set of connecting beams above and below the stiffening beam are replaced by a continuous uniform distribution of laminae with equivalent stiffness (Fig. 2). Assuming that the points of

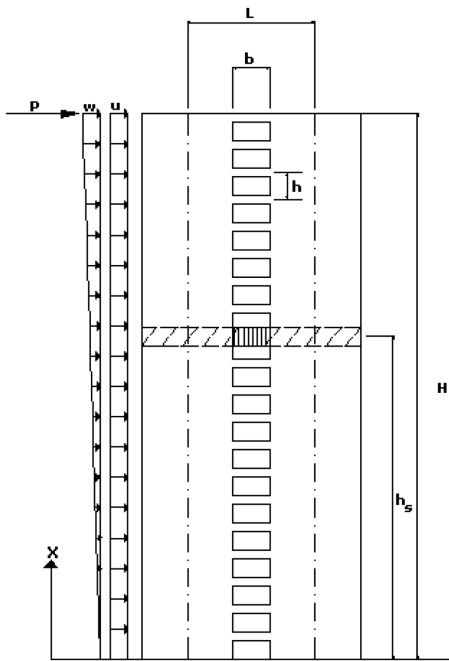


Fig. 1 Stiffened coupled shear walls

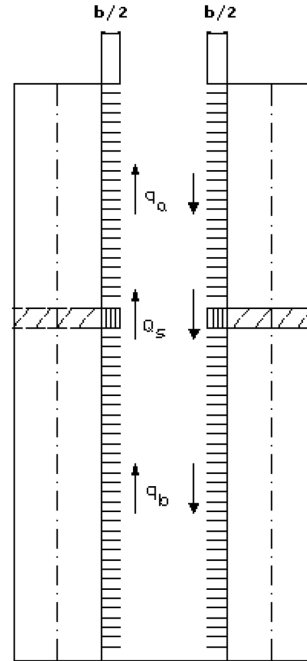


Fig. 2 Substituted structure

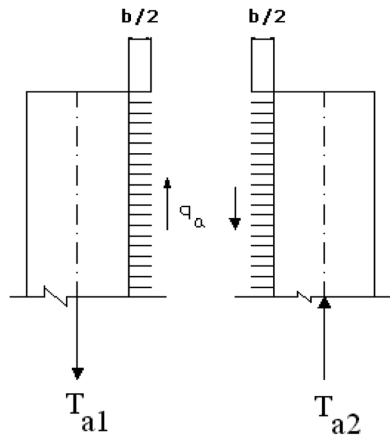


Fig. 3 The section above the stiffening beam

contraflexure of the connecting beams are in the mid-span and as the vertical displacement of the connecting beams in its middle section is zero, the following equations are obtained.

- At the section above the stiffening beam (See Fig. 3)

$$L \frac{dy_a}{dx} - \frac{hb^3}{12EI_b} q_a - \frac{1}{E} \left[\int_{h_s}^x \frac{T_{a1}}{A_1} dx + \int_{h_s}^x \frac{T_{a2}}{A_2} dx + \int_0^{h_s} \frac{T_{b1}}{A_1} dx + \int_0^{h_s} \frac{T_{b2}}{A_2} dx \right] = 0 \quad (1)$$

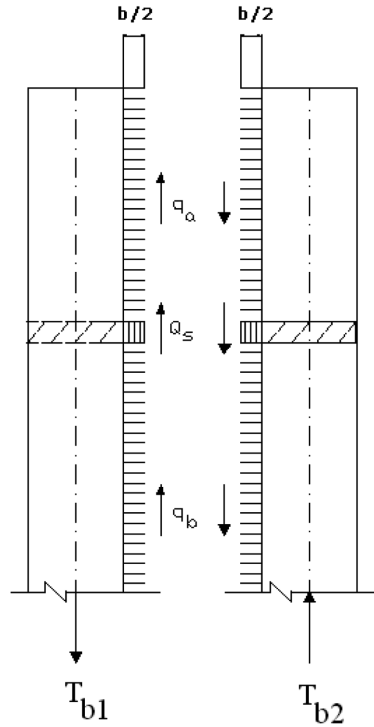


Fig. 4 The section below the stiffening beam

- At the section below the stiffening beam (See Fig. 4)

$$L \frac{dy_b}{dx} - \frac{hb^3}{12EI_b} q_b - \frac{1}{E} \left[\int_0^x \frac{T_{b1}}{A_1} dx + \int_0^x \frac{T_{b2}}{A_2} dx \right] = 0 \quad (2)$$

- In the stiffening beam

$$L \frac{dy}{dx} - \frac{Q_s b^3}{12E_s I_s} - \frac{1}{E} \left[\int_0^{h_s} \frac{T_{b1}}{A_1} dx + \int_0^{h_s} \frac{T_{b2}}{A_2} dx \right] = 0 \quad (3)$$

By equating the corresponding terms of Eqs. (1) or (2) at $x = h_s$, the shear force in the stiffening beam can be represented by

$$Q_s = S_m H q_{as} = S_m H q_{bs} \quad (4)$$

$$S_m = \frac{E_s I_s}{E I_b H / h} \quad (5)$$

In Eqs. (1) to (5), y_a, y_b are the lateral displacements of the wall and q_a, q_b are the laminar shears of connecting medium above and below the stiffening beam, respectively, T_{a1}, T_{a2} are the left and

right axial forces in the walls above the stiffening beam. Also, T_{b1} , T_{b2} are the left and right axial forces in the walls below the stiffening beam. L is the distance between centroidal axes of walls, b is clear span length of coupling beams, E , E_S are elastic moduli of walls and stiffening beam. A_1 , A_2 , I_1 and I_2 are the cross section areas and moment of inertia of the left and right walls. I_b and I_S are the moment of inertia of the coupling beam and the stiffening beam, respectively. q_{as} and q_{bs} are the laminar shear flows at $x = h_s$ and S_m is the relative flexural rigidity of the stiffening beam.

The three successive terms in the Eq. (1) are the relative displacement at the cut due to the bending of the walls, the deformation of the laminae and the axial deformation of the walls, respectively. By adapting the equilibrium equations for the longitudinal axis of the walls, the following relationships have been obtained for calculating the axial force of each wall at different sections:

- At the section above the stiffening beam

$$T_{a1} = \int_x^H q_a dx - \int_x^H P_{a1} dx \quad (6)$$

$$T_{a2} = \int_x^H q_a dx + \int_x^H P_{a2} dx \quad (7)$$

- At the section below the stiffening beam

$$T_{b1} = \int_{h_s}^H q_a dx + \int_x^{h_s} q_b dx + Q_S - \int_{h_s}^H P_{a1} dx - \int_x^{h_s} P_{b1} dx \quad (8)$$

$$T_{b2} = \int_{h_s}^H q_a dx + \int_x^{h_s} q_b dx + Q_S + \int_{h_s}^H P_{a2} dx + \int_x^{h_s} P_{b2} dx \quad (9)$$

In Eqs. (6) to (9), p_{a1} and p_{a2} are the left and right uniformly distributed axial loads in the walls above the stiffening beam, respectively, and p_{b1} and p_{b2} are the left and right uniformly distributed axial loads in the walls below the stiffening beam, respectively.

The moment-curvature relationships at x position will be obtained from the following equations as shown in Figs. 3, 4 and 5

$$EI \frac{d^2 y_b}{dx^2} = M_e - L \left(\int_{h_s}^H q_a dx + \int_x^{h_s} q_b dx + Q_S \right) + (P_{a1} + P_{a2}) \int_x^{h_s} y_a dx + (P_{b1} + P_{b2}) \int_x^{h_s} y_b dx \quad 0 \leq x \leq h_s \quad (10)$$

$$EI \frac{d^2 y_a}{dx^2} = M_e - L \int_x^H q_a dx + (P_{a1} + P_{a2}) \int_x^H y_a dx \quad h_s \leq x \leq H \quad (11)$$

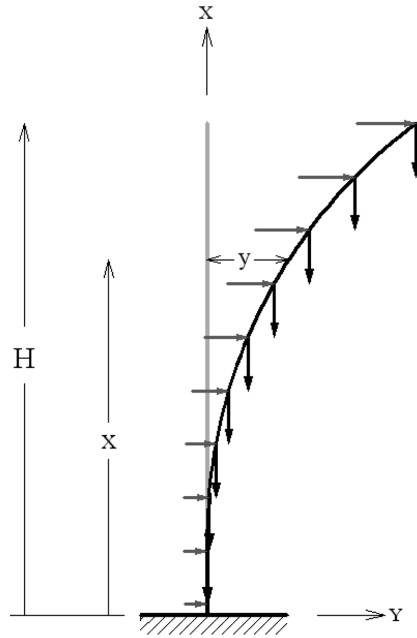


Fig. 5 The effect of uniformly distributed axial load on the structure

In the above equations, the moment caused by the external loading (M_e) can be calculated as follows

$$M_e = \frac{u}{2}(H-x)^2 + \frac{w}{6H}(2H^3 - 3H^2x + x^3) + p(H-x) \quad (12)$$

where u is the uniformly distributed load, w is the maximum intensity of triangularly distributed load on the top of the structure and p is the concentrated load on the top of the structure. Combining Eqs. (10) and (11) with Eqs. (6) to (9), the axial forces of the walls will be obtained as follows

$$T_{a1} = \frac{M_e}{L} + \frac{(P_{a1} + P_{a2})}{L} \int_x^H y_a dx - \frac{EI}{L} \frac{d^2 y_a}{dx^2} - \int_x^H P_{a1} dx \quad (13)$$

$$T_{a2} = \frac{M_e}{L} + \frac{(P_{a1} + P_{a2})}{L} \int_x^H y_a dx - \frac{EI}{L} \frac{d^2 y_a}{dx^2} + \int_x^H P_{a2} dx \quad (14)$$

$$T_{b1} = \frac{M_e}{L} + \frac{(P_{a1} + P_{a2})}{L} \int_{x_s}^H y_a dx + \frac{(P_{b1} + P_{b2})}{L} \int_x^{x_s} y_b dx - \frac{EI}{L} \frac{d^2 y_b}{dx^2} - \int_{x_s}^H P_{a1} dx - \int_x^{x_s} P_{b1} dx \quad (15)$$

$$T_{b2} = \frac{M_e}{L} + \frac{(P_{a1} + P_{a2})}{L} \int_{x_s}^H y_a dx + \frac{(P_{b1} + P_{b2})}{L} \int_x^{x_s} y_b dx - \frac{EI}{L} \frac{d^2 y_b}{dx^2} + \int_{x_s}^H P_{a2} dx + \int_x^{x_s} P_{b2} dx \quad (16)$$

3. The governing differential equations

Substituting the Eqs. (11), (13) and (14) into the second order derivative of Eq. (1) leads to the governing equation at the above section of the stiffening beam

$$\begin{aligned} \frac{d^5 y_a}{dx^5} - \left[\frac{12I_b}{hb^3 I} \left(L^2 + \frac{I}{A_1} + \frac{I}{A_2} \right) \right] \frac{d^3 y_a}{dx^3} + \frac{(P_{a1} + P_{a2})}{EI} \frac{d^2 y_a}{dx^2} \\ - \frac{12I_b(P_{a1} + P_{a2})}{hb^3 EI} \left(\frac{1}{A_1} + \frac{1}{A_2} \right) y_a + \frac{12I_b}{hb^3 EI} \left(\frac{1}{A_1} + \frac{1}{A_2} \right) \frac{dM_e}{dx} - \frac{1}{EI} \frac{d^3 M_e}{dx^3} + \frac{12I_b L}{hb^3 EI} \left(\frac{P_{a1}}{A_1} - \frac{P_{a2}}{A_2} \right) = 0 \end{aligned} \quad (17)$$

Also, substituting the Eqs. (10), (15) and (16) into the second order derivative of Eq. (2) leads to the governing equation at the below section of the stiffening beam

$$\begin{aligned} \frac{d^5 y_b}{dx^5} - \left[\frac{12I_b}{hb^3 I} \left(L^2 + \frac{I}{A_1} + \frac{I}{A_2} \right) \right] \frac{d^3 y_b}{dx^3} + \frac{(P_{b1} + P_{b2})}{EI} \frac{d^2 y_b}{dx^2} \\ - \frac{12I_b(P_{b1} + P_{b2})}{hb^3 EI} \left(\frac{1}{A_1} + \frac{1}{A_2} \right) y_b + \frac{12I_b}{hb^3 EI} \left(\frac{1}{A_1} + \frac{1}{A_2} \right) \frac{dM_e}{dx} - \frac{1}{EI} \frac{d^3 M_e}{dx^3} + \frac{12I_b L}{hb^3 EI} \left(\frac{P_{b1}}{A_1} - \frac{P_{b2}}{A_2} \right) = 0 \end{aligned} \quad (18)$$

To solve the governing Eqs. (17) and (18), a characteristic function of degree 5 has been obtained using MATLAB. Extracting a closed-form solution for these equations involves a complex process. Hence, equations of displacement at above and below sections of the stiffening beam have been determined by assigning the given values to the geometric parameters of the equations and applying the boundary conditions.

4. Boundary conditions

To determine the integration constants in the fifth order differential Eqs. (17) and (18) the following ten boundary conditions are employed:

- At the base level, $x = 0$ boundary conditions are

$$y_b|_{x=0} = 0 \quad (19)$$

$$\left. \frac{dy_b}{dx} \right|_{x=0} = 0 \quad (20)$$

- At the level of stiffening beam $x = h_s$, boundary conditions are

$$y_a|_{x=h_s} = y_b|_{x=h_s} \quad (21)$$

$$\left. \frac{dy_a}{dx} \right|_{x=h_s} = \left. \frac{dy_b}{dx} \right|_{x=h_s} \quad (22)$$

$$T_{a1}|_{x=h_s} + Q_s = T_{b1}|_{x=h_s} \quad (23)$$

$$q_a|_{x=h_s} = q_b|_{x=h_s} \quad (24)$$

$$\left\{ L \frac{d^2 y_a}{dx^2} - \frac{hb^3}{12EI_b} \frac{dq_a}{dx} - \frac{1}{E} \left(\frac{T_{a1}}{A_1} + \frac{T_{a2}}{A_2} \right) \right\} \Big|_{x=h_s} = \left\{ L \frac{d^2 y_b}{dx^2} - \frac{hb^3}{12EI_b} \frac{dq_b}{dx} - \frac{1}{E} \left(\frac{T_{b1}}{A_1} + \frac{T_{b2}}{A_2} \right) \right\} \Big|_{x=h_s} \quad (25)$$

• At the top of the structure $x = H$, boundary conditions are

$$T_{a1}|_{x=H} = 0 \quad (26)$$

$$\left. \frac{dq_a}{dx} \right|_{x=H} = 0 \quad (27)$$

$$L \left. \frac{dy_a}{dx} \right|_{x=H} - \frac{hb^3}{12EI_b} q_a|_{x=H} - \frac{1}{E} \left[\int_{h_s}^H \frac{T_{a1}}{A_1} dx + \int_{h_s}^H \frac{T_{a2}}{A_2} dx + \int_0^{h_s} \frac{T_{b1}}{A_1} dx + \int_0^{h_s} \frac{T_{b2}}{A_2} dx \right] = 0 \quad (28)$$

5. Numerical investigation

In order to obtain the optimal position of the stiffening beam considering the effect of axial force on the stiffened coupled shear walls supported on rigid foundation, a 20-story structure, as shown in Fig. 1, has been analysed as an example. The plan dimensions of the structure are shown in Fig. 6. The structure has been assumed to be subjected to a uniformly distributed load with an intensity of 15 kN/m along the height. Geometrical dimensions and structural properties have been chosen as follows:

$$\begin{array}{lll} H = 60 \text{ m}, & I_b = 0.002133 \text{ m}^4, & I_1 = 9.154 \text{ m}^4 \\ h = 3 \text{ m}, & I_s = 0.073233 \text{ m}^4, & I_2 = 33.33 \text{ m}^4 \\ A_1 = 2.6 \text{ m}^2 & E = E_s = 2.4 \times 10^7 \text{ kN/m}^2, & I = 42.487 \text{ m}^4 \\ A_2 = 4 \text{ m}^2, & L = 9.75 \text{ m}, & \rho = 2400 \text{ kg/m}^3 \end{array}$$

In order to investigate how the wall's height influences the optimal position of the stiffening beam considering the effect of axial force, the height of the structure studied in example has been doubled and tripled (equivalent to the height of 40 and 60 stories structure) and results of analysis are presented in Figs. 7 to 12.

As shown in Figs. 7 to 12, the effect of axial force on the stiffened coupled shear walls causes an increase in the maximum displacement at the top and the maximum bending moment at the bottom of the building. Figs. 7 to 9 and 10 to 12 show respectively the variation of the top lateral deflection

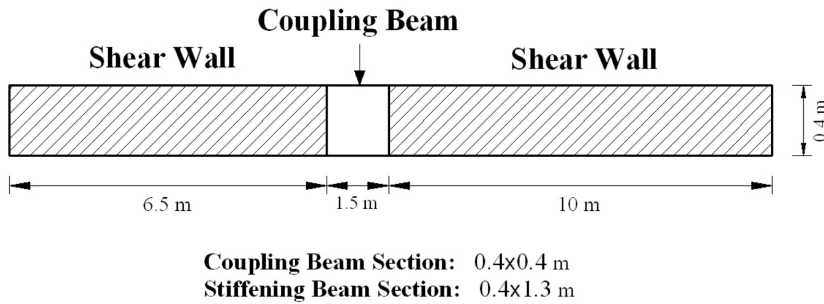


Fig. 6 Dimensions of example structure

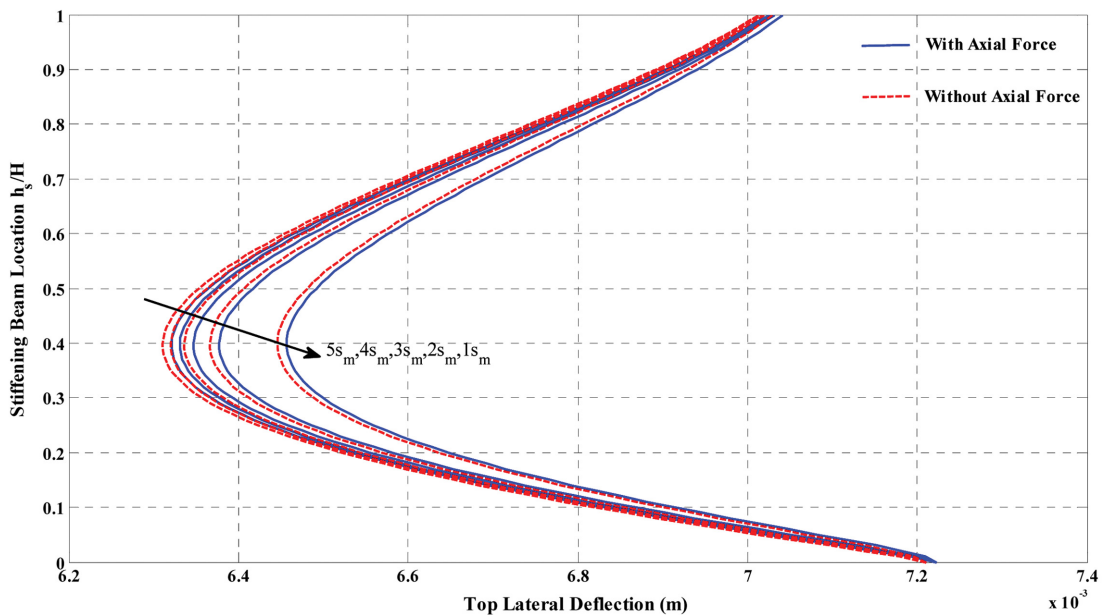


Fig. 7 Effect of stiffening beam location on top lateral deflection for 20 story structure

and the base bending moment in walls with and without considering the effect of axial force. These figures, which present the results of analyzing 20-, 40-, and 60-story structures, show the variation of above-mentioned parameters against the stiffening beam location, h_s/H , for different flexural rigidities of stiffening beam ($1S_m$ to $5S_m$). It can be seen that with increasing the height of the walls, the optimal position of the stiffening beam moves downward in both cases with and without considering the effect of axial force.

The selection of the optimum location for installing the stiffening beam depends on achieving either the condition for the minimum value of the base bending moment or the top lateral deflection. The increase in the rigidity of stiffening beam leads to the considerable decrease in the lateral deflection and the base bending moment in the walls. It is also shown that by increasing the height of the walls, the effect of axial force becomes more significant.

The taller buildings, the greater the inertia that must be provided by the stiffening beam to achieve the same relative reduction in the top lateral deflection and the base bending moment. As

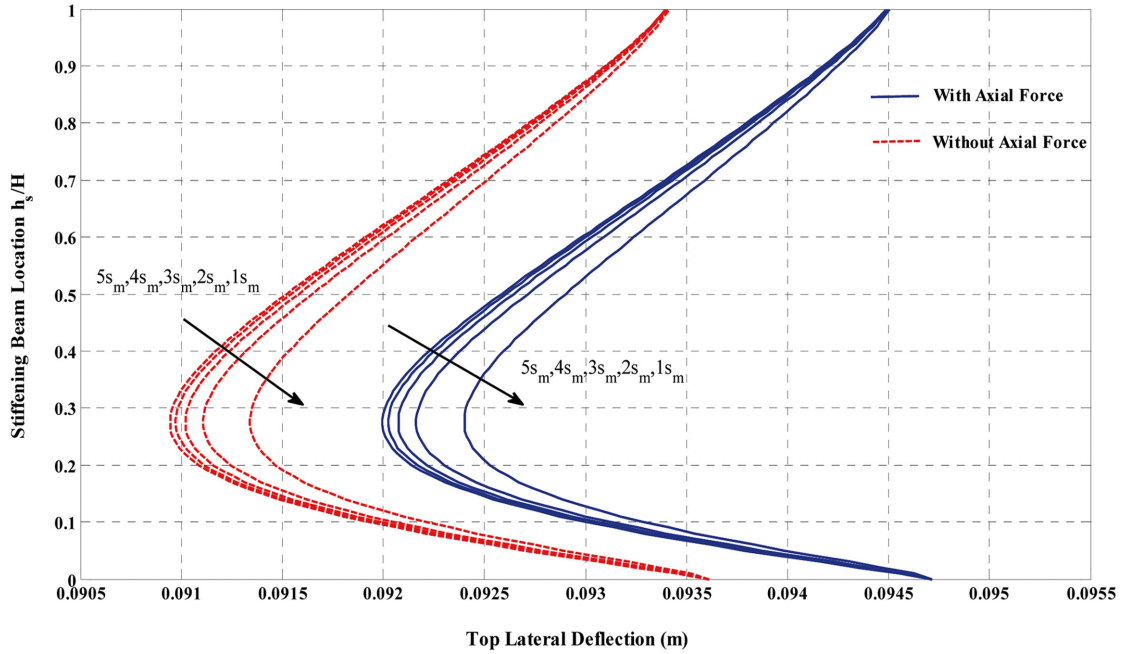


Fig. 8 Effect of stiffening beam location on top lateral deflection for 40 story structure

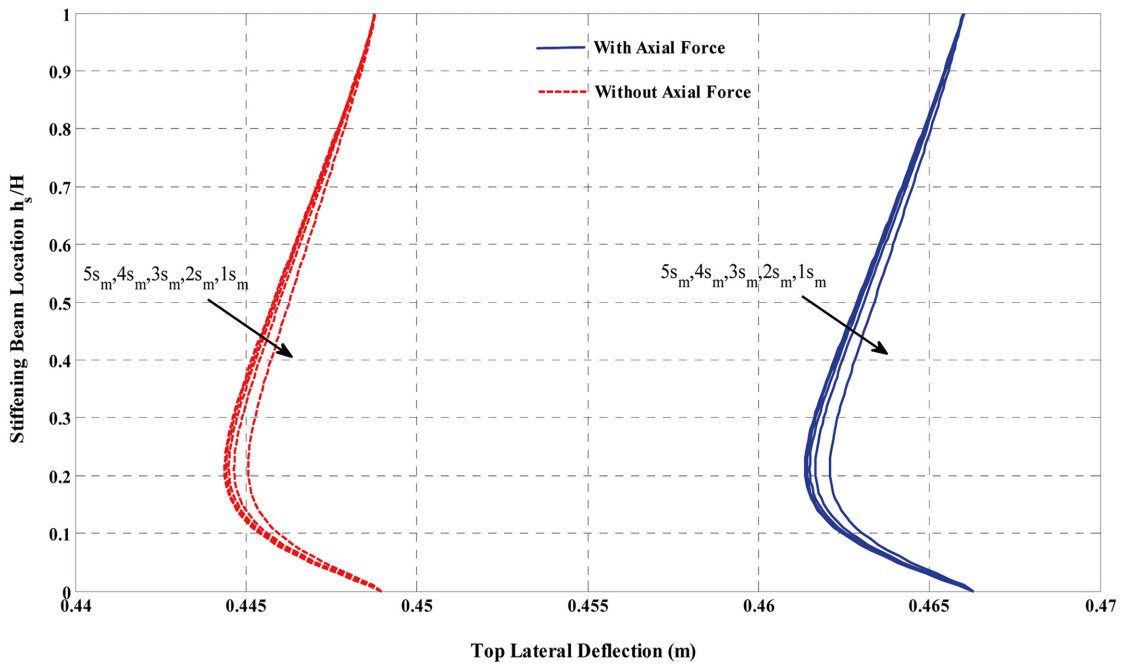


Fig. 9 Effect of stiffening beam location on top lateral deflection for 60 story structure

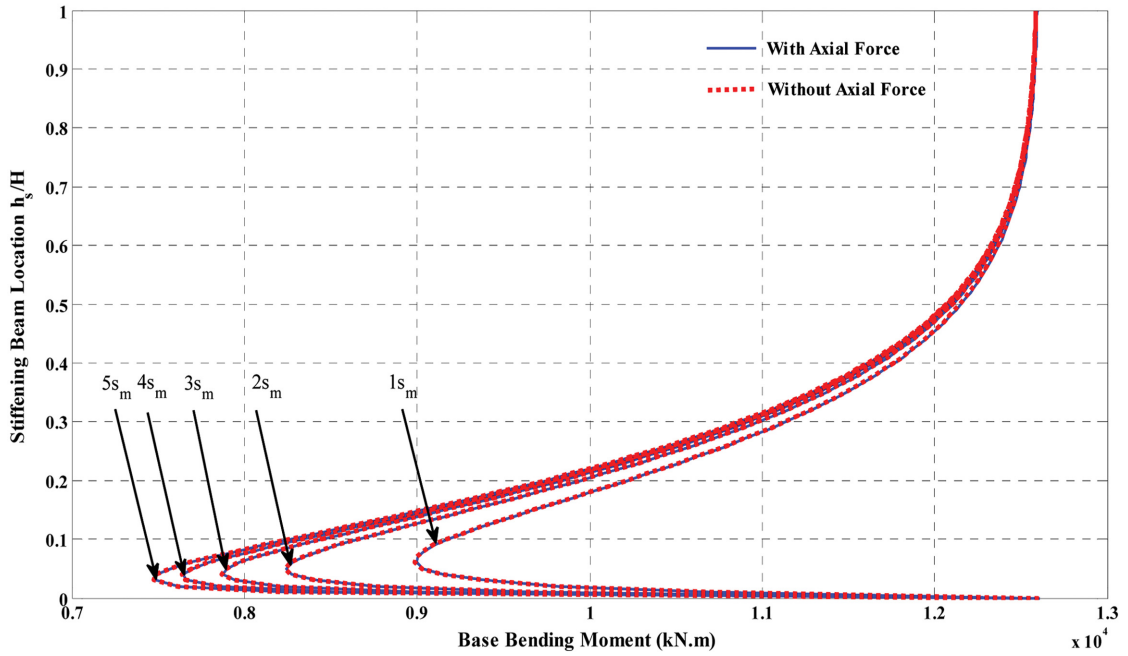


Fig. 10 Effect of stiffening beam location on base bending moment in the walls for 20 story structure

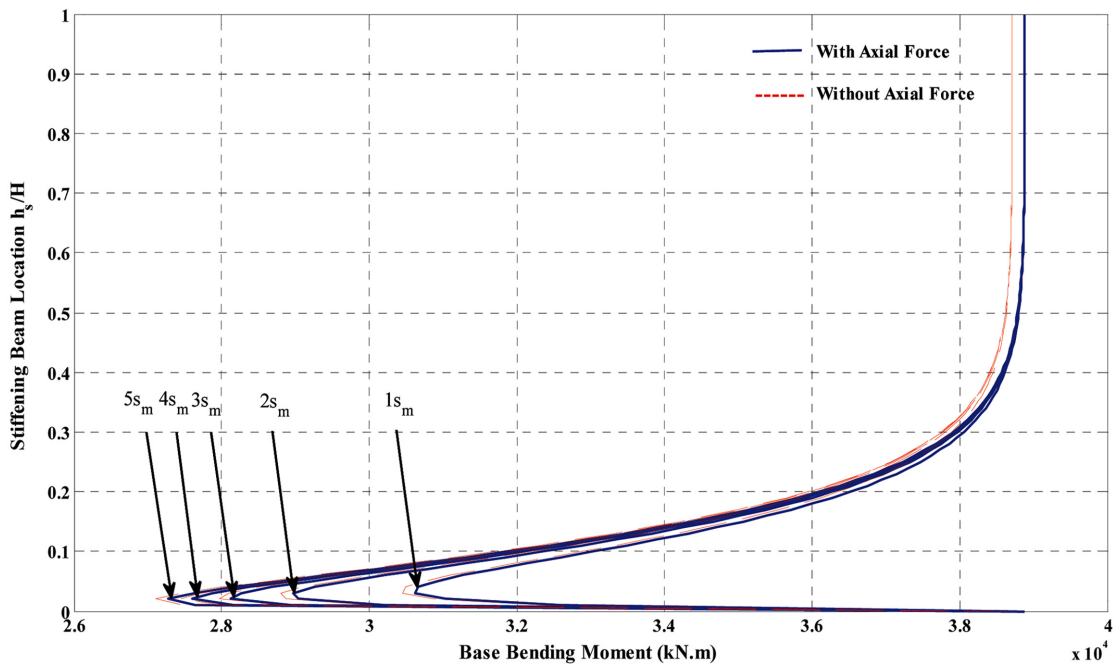


Fig. 11 Effect of stiffening beam location on base bending moment in the walls for 40 story structure

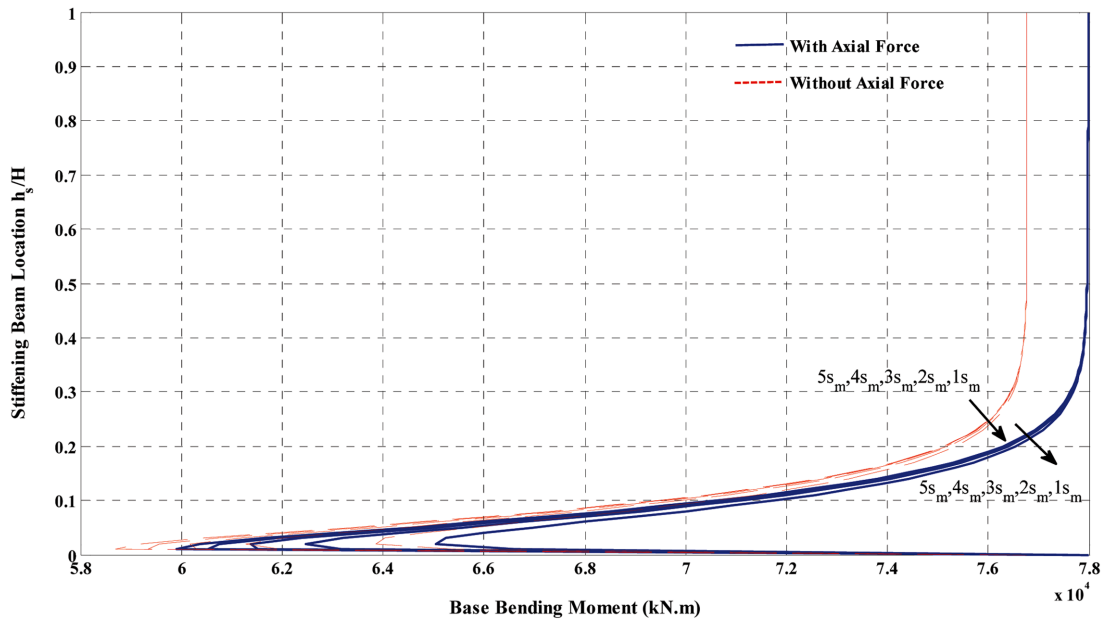


Fig. 12 Effect of stiffening beam location on base bending moment in the walls for 60 story structure

indicated, the optimal position of the stiffening beam is dependent on the I_s/I_b ratio. Since the flexural rigidity of the stiffening beam is much greater than the rigidity of the coupling beam, the change of the flexural rigidity of the stiffening beam has little effect on the optimal position which is not considerable. However, with considerably small rigidity ratios, the optimal position of the stiffening beam will change remarkably.

6. Conclusions

In this paper, based on the continuum approach, the optimal position of the stiffening beam on the stiffened coupled shear walls is investigated considering the effect of uniformly distributed axial loads. The presented method also investigates the effect of the height of stiffened coupled shear walls on the optimal position of the stiffening beam with and without considering the axial force effect. In the research efforts expended so far on determining the optimal position of the stiffening beam, the effect of axial force has not been considered. In a tall building, weight induced axial force can affect the behavior of the structure. Hence, it is essential to develop a method which includes the effect of axial force.

Results indicate that with increasing the height of the walls, the optimal position of the stiffening beam moves downward in both cases with and without considering the effect of axial force. The results also verify the fact that the effect of axial force of stiffened coupled shear walls increases the lateral deflection and the base bending moment in the walls. Furthermore, it is observed that by increasing the height of the walls, the effect of axial force becomes more significant.

By increasing the flexural rigidity of the stiffening beam, curves corresponding to the top lateral deflection and the base bending moment in walls become closer. Increasing the flexural rigidity,

beyond a specific value, does not have any considerable effect on the top lateral deflection and accordingly has little influence on the optimal position of the stiffening beam. The difference between the optimal positions in cases with and without considering the axial force effect is not noticeable.

The increase in the rigidity of stiffening beam leads to the considerable decrease in the lateral deflection and the base bending moment in the walls. Three advantages of the proposed method are the acceptable accuracy, simplicity of its data, and the extremely decreased computation time. The mentioned advantages lead the proposed method to an effective method for the pre-design of high-rise buildings.

References

- Aksogan, O., Arslan, H.M. and Akavci, S.S. (2003), "Stiffened coupled shear walls on elastic foundation with flexible connections and stepwise changes in width", *Iran. J. Sci. Technol.*, **27**(B1), 37-46.
- Aksogan, O., Bikce, M., Emsen, E. and Arslan, H.M. (2007), "A simplified analysis of multi-bay stiffened coupled shear walls", *Adv. Eng. Softw.*, **38**, 552-560.
- Arslan, H.M., Aksogan, O. and Akavci, S.S. (2001), "Stiffened coupled shear walls on elastic foundations with flexible connections and stepwise changes in width", *Turkish J. Eng. Environ.*, **25**, 517-526.
- Arslan, H.M., Aksogan, O. and Choo, B.S. (2004), "Free vibrations of flexibly connected elastically supported stiffened coupled shear walls with stepwise changes in width", *Iran. J. Sci. Technol.*, **28**(B5), 605-614.
- Bikce, M., Aksogan, O. and Arslan H.M. (2004), "Stiffened multi-bay coupled shear walls on elastic foundation", *Iran. J. Sci. Technol.*, **28**(B1), 43-52.
- Bozdogan, K.B., Ozturk, D. (2008), "A method for static and dynamic analyses of stiffened multi-bay coupled shear walls", *Struct. Eng. Mech.*, **28**(4), 479-489.
- Chan, H.C. and Kuang, J.S. (1989a), "Stiffened coupled shear walls", *J. Eng. Mech. ASCE*, **115**(4), 689-703.
- Chan, H.C. and Kuang, J.S. (1989b), "Elastic design charts for stiffened coupled shear walls", *J. Struct. Eng. ASCE*, **115**(2), 247-267.
- Choo, B.S. and Coull, A. (1984), "Stiffening of laterally loaded coupled shear walls on elastic foundations", *Build. Environ.*, **19**, 251-256.
- Choo, B.S. and Li, G.Q. (1997), "Structural analysis of multi-stiffened coupled shear walls on flexible foundations", *Comput. Struct.*, **64**(1-4), 837-848.
- Coull, A. and Bensmail, L. (1991), "Stiffened coupled shear walls", *J. Struct. Eng. ASCE*, **117**(8), 2205-2223.
- Coull, A. (1974), "Stiffening of coupled shear walls against foundation movements", *Struct. Eng.*, **52**(1), 23-26.
- Emsen, E., Turkozer, C.D., Aksogan, O., Resatoglu, R. and Bikce, M. (2009), "Non-planar coupled shear walls with stiffening beams", *Sci. Res. Essay.*, **4**(4), 328-345.
- Hadidi, A., Farahmand Azar, B. and Khosravi, H. (2011), "An investigation on the behavior of stiffened coupled shear walls considering axial force effect", *Struct. Des. Tall Build.* (in revised).
- Kuang, J.S. and Chau, C.K. (1998), "Free vibration of stiffened coupled shear walls", *Struct. Des. Tall Build.*, **7**, 135-145.
- Matlab V7.1 (2004), Users Manual, Mathworks Inc., USA.
- Zeidabadi, N.A., Mirtalae, K. and Mobasher, B. (2004), "Optimized use of the outrigger system to stiffen the coupled shear walls in tall buildings", *Struct. Des. Tall Special Build.*, **13**, 9-27.

Notations

A_1, A_2	Cross-sectional area of walls 1 and 2, respectively
b	Clear span length of coupling beams
E, E_S	Elastic moduli of walls and stiffening beam, respectively
H	Total height of structure
h	Height of story
h_s	Position of stiffening beam
I_1, I_2	Second moment of area of walls 1 and 2, respectively
I	Total second moment of area of walls 1 and 2
I_b, I_S	Second moment of area of coupling beam and of stiffening beam, respectively
L	Distance between centroidal axes of walls
M_e	Bending moment due to external loads
M_1, M_2	Bending moments in walls
M_0	Bending moments in walls at base level
P	Concentrated load at top of structure
p_{a1}, p_{a2}	Left and right uniformly distributed axial loads in the walls above the stiffening beam, respectively
p_{b1}, p_{b2}	Left and right uniformly distributed axial loads in the walls below the stiffening beam, respectively
Q_S	Shear forces in stiffening beam
q_a, q_b	Laminar shear of connecting medium above and below the stiffening beam, respectively
S_m	Relative flexural rigidity of stiffening beam
T_{a1}, T_{a2}	Left and right axial forces in the walls above the stiffening beam, respectively
T_{b1}, T_{b2}	Left and right axial forces in the walls below the stiffening beam, respectively
u	Intensity of uniformly distributed load
w	Maximum intensity of triangularly distributed load
x	Height coordinate
y_a, y_b	Lateral deflection of the wall above and below the stiffening beam, respectively
y_H	Top lateral deflection
ρ	Mass density